Published in final edited form as:

J Magn Reson. 2018 October ; 295: 80–86. doi:10.1016/j.jmr.2018.08.002.

Determination of binding affinities using hyperpolarized NMR with simultaneous 4-channel detection

Yaewon Kim[#], **Mengxiao Liu**[#], and **Christian Hilty**[*]

Chemistry Department, Texas A&M University, 3255 TAMU, College Station, TX 77843, USA

[#] These authors contributed equally to this work.

Abstract

Dissolution dynamic nuclear polarization (D-DNP) is a powerful technique to improve NMR sensitivity by a factor of thousands. Combining D-DNP with NMR-based screening enables to mitigate solubility or availability problems of ligands and target proteins in drug discovery as it can lower the concentration requirements into the sub-micromolar range. One of the challenges that D-DNP assisted NMR screening methods face for broad application, however, is a reduced throughput due to additional procedures and time required to create hyperpolarization. These requirements result in a delay of several tens of minutes in-between each NMR measurement. To solve this problem, we have developed a simultaneous 4-channel detection method for hyperpolarized ^{19}F NMR, which can increase throughput four-fold utilizing a purpose-built multiplexed NMR spectrometer and probe. With this system, the concentration-dependent binding interactions were observed for benzamidine and benzylamine with the serine protease trypsin. A T_2 relaxation measurement of a hyperpolarized reporter ligand (TFBC; $CF_3C_6H_4CNHNH_2$), which competes for the same binding site on the trypsin with the other ligands, was used. The hyperpolarized TFBC was mixed with trypsin and the ligand of interest, and injected into four flow cells inside the NMR probe. Across the set of four channels, a concentration gradient was created. From the simultaneously acquired relaxation datasets, it was possible to determine the dissociation constant (K_D) of benzamidine or benzylamine without the requirement for individually optimizing experimental conditions for different affinities. A simulation showed that this 4-channel detection method applied to D-DNP NMR extends the screenable K_D range to up to three orders of magnitude in a single experiment.

1. Introduction

Advances in hyperpolarization, including using the methods of dissolution dynamic nuclear polarization (D-DNP)[1,2] or parahydrogen induced polarization (PHIP)[3,4] hold promise to improve the capabilities of liquid state NMR spectroscopy for chemical analysis. These techniques lower the limits of detection by orders of magnitude, thereby providing access to conditions, where otherwise prohibitive signal averaging would be required.[5,6] The time requirements for preparing hyperpolarized (HP) samples, however, partially offset these gains for routine applications. In particular, quantitative problems frequently require the

[*]corresponding author. chilty@tamu.edu.

acquisition of multiple spectra in function of a variable parameter. For example, titrations are commonly used for the determination of binding affinities such as between proteins and ligands in drug discovery.[7] They are applied to the measurement of equilibrium constants in complex molecules, such as the protonation or deprotonation of amino acid side chains accompanied by a structural change in a protein,[8] or in combination with relaxation measurements for the characterization of dynamic changes that occur due to intermolecular interactions.[9–11]

These problems require multiple data acquisitions, resulting in increased complexity for the application of hyperpolarization protocols that include several additional preparation steps. For D-DNP, hyperpolarization itself may require microwave irradiation for a duration of on the order of tens of minutes to hours, in addition to mechanical steps for sample loading and dissolution.[12] High throughput D-DNP NMR has been proposed with the construction of instrumentation that can polarize multiple sample aliquots at the same time, followed by sequential dissolution.[13–16] Experiments may also be facilitated by developing NMR pulse sequences and data analysis techniques that reduce the number of required repetitions for a specific problem. Authors of this publication have previously developed such methods for the characterization of protein-ligand interactions, employing relaxation measurements of a reporter ligand.[17] These methods were subsequently applied in combination with a purpose developed NMR probe, which allowed the simultaneous measurement of two relaxation traces from a single HP aliquot.[18]

Here, we demonstrate that up to four simultaneous measurements of concentration-dependent relaxation data can be achieved with a probe designed to fit into a standard narrow-bore magnet, and a spectrometer with a split excitation channel capable of applying the same pulse sequence on each channel. Using the protein trypsin in combination with several ligands, we show that binding affinity can be determined over a range of three orders of magnitude in a single experiment. Finally, we include a detailed analysis of the accuracy of the method and discuss applicability to multi-scan NMR in general.

2. Materials and methods

2.1 Four-channel NMR spectrometer and probe

A four-channel NMR spectrometer for ^{19}F detection was built on four radio frequency (RF) generation and processing boards, one of which was a RadioProcessor™ (RP), and the others were receiver-only RP (RP-RX) boards (SpinCore Technologies, Gainesville, FL). The RF signal generated from the only excitation channel (RP) was first amplified by a power amplifier (model BT00250 Gamma, Tomco Technologies, Stepney, South Australia). The amplified RF signal was then fed into power splitters (model ZA2CS-62–40W+, Mini-Circuits, Brooklyn, NY) where four RF outputs were produced and transmitted to the four coils in the probe. In the receiver part, all four boards were utilized, receiving the induced NMR signals separately. See the Supporting Information for a detailed description (Figure S1).

The multiplexed NMR probe, accommodating four flow cells, was designed to fit into a standard narrow-bore magnet (40 mm accessible diameter within the shim stack). The probe

expands on a previous two-channel design.[18] Briefly, U-shaped flow cells of 100 μL volume were stacked within 35 mm of vertical space with a center-to-center distance of 8 mm (Figure S2). Solenoidal RF coils, wound around the flow cells, were arranged orthogonally to each other to reduce cross-talk, and grounded copper sheets (0.55 mm thickness) were inserted in-between for RF shielding. Each coil was tuned to the ^{19}F NMR frequency at 9.4 T (376.4 MHz) by using a remote tuning and matching circuit.[19] The cross-talk between individual channels was measured by applying a radio-frequency pulse to, and acquiring NMR signal from a channel that was empty, while one of other three channels was filled with a solution of 130 mM trifluoroethanol (TFE). The channels that were not involved in the measurement were terminated with 50 ohms. With this method, 1–5% cross-talk was observed between neighboring channels. The cross-talk from non-adjacent coils was less than 1%.

2.2 Sample preparation

A solution of 10 mM 4-(trifluoromethyl)benzene-1-carboximidamide hydrochloride hydrate (TFBC·HCl; Maybridge, U.K.) for hyperpolarization was prepared in a mixture of D_2O/DMSO-d_6 (v/v 1:1) with 30 mM 4-hydroxy-2,2,6,6-tetramethylpiperidine-1-oxyl (TEMPOL; Sigma-Aldrich, St. Louis, MO). Non-HP samples contained 5 μM trypsin (AMRESCO, Road Solon, OH) in buffer (50 mM Tris, 10 mM $CaCl_2$, 50 mM trifluoroacetic acid (TFA), pH 8). The compound TFA was used as an internal reference to evaluate the dilution factor (DF) of the non-HP sample component in the final solution. For the measurements of concentration-dependent relaxation data, solutions of 37.5, 375, 1875, and 3750 μM benzylamine (TCI, Portland, OR) and benzamidine (Sigma-Aldrich, St. Louis, MO) were prepared with 5 μM trypsin in the same buffer. The concentrations of stock solutions were determined by UV/Vis and NMR spectroscopy.

2.3 Hyperpolarization

A 10-μL aliquot of TFBC sample was loaded into a HyperSense DNP polarizer (Oxford Instruments, Abingdon, U.K.) operating at 1.4 K. Hyperpolarization on ^{19}F spins of the sample was achieved by microwave irradiation of 94.055 GHz and 100 mW power for 20 min. After being dissolved in a degassed buffer (50 mM Tris and 10 mM $CaCl_2$ at pH 8), pre-heated to approximately 385 K, the sample was injected into the flow cells through a flow path described in the following section.

2.4 Simultaneous sample mixing and injection

The flow path was designed to split a single stream of HP sample into four substreams. Each substream was mixed with another reagent individually before filling the flow cells, as depicted in Figure 1a. For flow injection, high-pressure syringe pumps (Pump A; 500D and Pump B; 1000D Teledyne Isco, Lincoln, NE) were enabled before the dissolution of a hyperpolarized sample. A steady liquid pressure was achieved by flowing water through an open path to waste (see figure). Nominal flow rates were 160 and 150 mL/min for pump A and B, respectively. Following the dissolution, when the HP sample arrived in the sample loop (l1), the injection valve (v1) was switched, and the HP sample was driven to flow into the splitters. After 400 ms, the second valve (v2) was switched, allowing the non-HP samples to flow and admix to the HP samples. After running simultaneously for 500 ms,

both pumps were stopped. The NMR measurement began after 400 ms of sample settling time.

The non-HP reagents including protein or protein and ligand of interest were manually filled into the separate sections of tubing (t6, V = 40 μL) before the start of the dissolution. The inlets and outlets of these sections were blocked using shut-off valves and plugs to hold the samples for each channel during the operation of Pump A. At every junction, Y-mixers (IDEX Health & Science, Oak Harbor, WA) were used, and check valves (IDEX Health & Science, Oak Harbor, WA) were installed to prevent back- or cross-flow.

The amount of sample delivered to the flow cells was estimated by measuring the DF of the reference compounds from one-pulse NMR measurements. The DF for HP samples was found from multiple test measurements where a solution of 50% TFE was loaded into the DNP polarizer. The pre-determined DF values were then used to estimate the concentrations of HP samples in four channels in the actual ligand binding experiments. The non-HP samples contained TFA in all experiments, whereby the concentrations of protein or competitive ligand were obtained from every injection based on the TFA signals. The DF determined from the individual channels averaged 450 ± 32 and 7.8 ± 1.0 for the HP and non-HP samples, respectively, with less than 10% variations in each channel (Table 1). A comparison between the DF from the four channels showed 20% and 35% variations for the HP and non-HP samples, respectively, which were taken account of in error analysis.

2.5 NMR spectroscopy

For four simultaneous measurements of transverse relaxation rate (R_2), a chemical shift resolved spin relaxation measurement was implemented using a Carr Purcell Meiboom Gill (CPMG) pulse sequence.[18,20] As shown in Figure 1b, the RF pulses were generated from a single excitation channel and fed into each coil after being split into four channels. Spin echo signals arising from the sample were received in separate receiver channels. A total of 860 spin echoes were acquired from each channel. Each echo was composed of 280 complex data points collected for 7 ms during the interpulse delay 2τ = 8 ms. The excitation pulse was set to 13.5 μs, which was the average of 90° pulse lengths measured to be 13, 13.5, 13 and 14 μs from the four channels, at a pulse power of 9.1 W ± 3% per channel. The transmitter offset frequency was set to the center frequency of the TFBC signals obtained from the four channels, as a slight difference in magnetic fields was present between the coils. In the one-pulse measurements for determining sample concentrations, 32 scans of ^{19}F NMR spectra were measured using a 90° pulse after the hyperpolarization was lost. The signal intensity was then converted to the sample concentrations in the flow cells, based on the calibration curves obtained from the individual channels.

2.6 Data analysis

Spin-echo signals from the relaxation measurements were processed by first applying a sine-squared window function with the center of the echo set to $t = 0$. After a complex-valued Fourier transformation, the spectra were phase corrected to minimize the imaginary part. Signal intensities, integrated over the signal range in the spectra, were fitted to a single exponential decay function to find a R_2 relaxation rate.

An increase in the R_2 relaxation rate of a ligand in the presence of protein reflects the ligand binding. When the ligand is in fast exchange with respect to the R_2 relaxation, the observed R_2 relaxation rate ($R_{2,\mathrm{obs}}$) is determined by Eq. (1):[21,22]

$$R_{2,obs} = (1 - pb)R_{2,f} + pbR_{2,b} + pb(1 - pb)^2\Delta\omega^2/k_{off} \quad \text{Eq. (1)}$$

$$\approx pb\left(R^*_{2,b} - R_{2,f}\right) + R_{2,f},\ where\ R^*_{2,b} = R_{2,b} + \Delta\omega^2/k_{off} \quad \text{Eq. (2)}$$

where pb is the fraction of bound ligands, $R_{2,\mathrm{f}}$ and $R_{2,\mathrm{b}}$ are R_2 relaxation rates of free and bound ligands, respectively, $\Delta\omega$ is a chemical shift difference between free and bound ligands, and k_{off} is the dissociation rate constant. Under the condition that $(1\text{-}pb)^2 \approx 1$, $R_{2,\mathrm{obs}}$ becomes linearly related to pb as expressed in Eq. (2).[23] When the ligand competes with another ligand for the same binding pocket in the protein, the system shifts to a new equilibrium, resulting in a change in pb and therefore $R_{2,\mathrm{obs}}$. The equation for pb under binding competition can be written in terms of protein and ligand concentrations and binding affinities of the two ligands.[24] In our experiments, TFBC was a reporter ligand whose K_{D} was known as 142 μM at pH 8.[23] Using the equations given in ref. [24] and knowledge of $R_{2,\mathrm{f}}$, $R_{2,\mathrm{b}}$*, as well as the concentrations of protein and ligands, the K_{D} of a competing ligand was found from four $R_{2,\mathrm{obs}}$ values measured in one experiment.

3. Results and discussion

The experiments utilized hyperpolarization of ^{19}F spins of a reporter ligand to evaluate the binding affinity of a ligand of interest based on the transverse relaxation rates (R_2) of the reporter ligand under the competitive binding. Figure 2 shows the concentration-dependent relaxation data obtained from the four simultaneous relaxation measurements performed with the multi-channel DNP-NMR. The hyperpolarized reporter ligand TFBC was injected into the four channels after mixing with the protein trypsin and known inhibitor benzamidine.[17] Trypsin was at a nominally equal concentration in each channel, whereas the concentration of benzamidine increased from the channel 1 to 4. The first 50 spin-echoes acquired from the four channels are shown in Figure 2a. Among the four echo trains, the signals from the channel 1 exhibit the fastest decay. The channels with higher numbers show a reduced signal decay rate due to a higher concentration of benzamidine, the ligand for which K_{D} was intended to be determined by the experiment, and which displaces the reporter ligand from the binding site. As seen from the graph in Figure 2b, the benzamidine concentrations varied from 1- to 10-, 50-, and 100-fold dilution of a 0.5 mM solution, and the average concentration of trypsin was 640 nM with a variation of 10% across the channels. The averaged concentration of reporter ligand in four channels was 22.3 μM. From the contour plots of Fourier-transformed frequency spectra shown in Figure 2c-f, the effect of benzamidine on the signal decay rates of the reporter ligand can be seen more clearly. The signal in each spectrum originates from the reporter ligand under fast exchange between the free and bound forms. Using an exponential fit to these signal intensities, the observed

relaxation rate constant ($R_{2,obs}$) for each channel was obtained. Without any modification to the experimental parameters such as sample concentrations, the relaxation experiment was conducted for a second ligand, benzylamine, which has a higher binding affinity than benzamidine (Figure S3).

The resulting $R_{2,obs}$ values of TFBC under competition with benzamidine and benzylamine are plotted with circles in Figures 3a and b, respectively. At all concentrations, a higher $R_{2,obs}$ is found with benzylamine compared to with benzamidine, which is explained by the relative binding strength of the two ligands. In the same trend, the fitting errors for $R_{2,obs}$, represented by error bars in the figure, from the benzylamine experiment are higher, which is attributed to fewer data points contributing to the data fitting for fast-relaxing signals (higher $R_{2,obs}$).

To determine K_D from four simultaneously measured $R_{2,obs}$ values, parameters including R_2 values of reporter ligand in free and bound states ($R_{2,f}$ and $R_{2,b}$*), concentrations of protein and ligands in each channel, and K_D of reporter ligand are required. The R_2 references were determined from separate measurements with the hyperpolarized reporter ligand (TFBC) in the absence and the presence of a known amount of trypsin. From three repetitions for each measurement, the average $R_{2,f}$ and $R_{2,b}$* for the four channels was found to be 0.66 ± 0.02 s^{-1} and 841 ± 82 s^{-1}, respectively. For the determination of $R_{2,b}$*, the fraction of bound TFBC (*pb*) was first calculated based on the known values of K_D of TFBC and the concentrations of TFBC and trypsin. Then, it was used to calculate $R_{2,b}$* using (Eq. 2) with the $R_{2,obs}$ and $R_{2,f}$ rates obtained from the measurements. The averaged values of $R_{2,f}$ and $R_{2,b}$* were assumed the same for all channels in the data analysis. Individually measured values are summarized in Table 2. A variation of about 10% in the $R_{2,b}$* values was observed from the four channels, which may be caused by different rf-pulse (B_1) or main field (B_0) distributions. With the final sample concentrations, which were 22.3 μM for TFBC and 0.66 μM for trypsin on average, the dissociation constant of the competing ligand was found by the fitting of the $R_{2,obs}$ values. From the datasets shown in Figure 3, K_D for benzamidine and benzylamine were determined to be 21.6 μM and 205 μM, respectively.

To provide error estimates for K_D that combine all the uncertainties present, Monte Carlo simulations were performed. First, 10^4 parameter sets were generated, each of which was composed of the measured relaxation rates ($R_{2,f}$, $R_{2,b}$*, and $R_{2,obs}$) and the concentrations of trypsin and two competing ligands. The assumptions made for this simulation are (1) $R_{2,f}$ and $R_{2,b}$* values are normally distributed about their corresponding value of the averaged R_2 with a relative standard deviation of 2.5% and 9.7%, respectively (see Table 2). (2) $R_{2,obs}$ values are normally distributed about the fitted $R_{2,obs}$ with a standard deviation obtained from each individual fit (fitting error). (3) Sample concentrations are normally distributed about the measured values with a relative standard deviation of 5%. (4) The binding affinity of reporter ligand is known exactly as K_D = 142 μM[23]. From the combinations of these simulated parameters, a distribution of K_D values was obtained. It was found that the 95% confidence intervals of K_D determined for benzamidine and benzylamine from a single measurement were (12.0 μM, 36.1 μM) and (136 μM, 327 μM), respectively. The K_D values and the associated error ranges obtained from additional experiments are summarized in Table 3. The table shows that the results are reproducible with less than 4% of the relative

standard deviation. The K_D values can be found by an alternative method, where $R_{2,b}$* and K_D are determined simultaneously from the datasets of the reference experiments and the competitive binding experiments. Using this method, the values of $R_{2,b}$* and K_D were found to be identical to the above within the error limits. An advantage of first determining $R_{2,b}$*, as described above, is that the reference datasets do not need to be fitted for every K_D determination.

We have further assessed the uncertainties in the K_D determination for wide-ranging affinities of a competing ligand from 10^{-2} to 10^4 μM. The data points shown in Figure 4a are examples of R_2 values from the artificial datasets created for seven selected K_D values at given concentrations similar to the experimental condition. For each case, a total of 10^4 values for R_2 were generated assuming that the R_2 values are normally distributed about the value of R_2 calculated using (Eq. 2) with a standard deviation equal to 6% of the calculated R_2 value. This error range was decided on based on the fitting errors obtained from all of the measured relaxation datasets. Except for this modification to the assumption (3) made above, the same assumptions were applied to the simulations. The uncertainties accumulated through the sequential K_D determination steps are indicated in Figure 4b using the error bars encompassing central 95% of the K_D distributions. It was found that K_D can be determined with a similar level of error to that observed for the K_D values of benzamidine and benzylamine over three orders of magnitude, from 10^0 to 10^2 μM. The error becomes significant when $K_D \geq 10^3$ μM or $K_D \leq 10^{-1}$ μM, where the width of the 95% confidence interval exceeds the true K_D value by 20-fold. Additionally, it was found that the most significant source of error is $R_{2,b}$*. This uncertainty can be reduced through multiple measurements of this reference value. In the absence of $R_{2,b}$* error, the confidence intervals for K_D would be reduced approximately by half.

It has been previously shown that it is possible to obtain an accurate K_D from a single- or two-point R_2 measurement with competitive binding using D-DNP.[17,18] The four-channel NMR apparatus described here covers a broadened range of screenable K_D over three orders of magnitude compared to the previous experiments. It effectively permits the use of a single experiment without individual optimization of experimental conditions. A challenge in using multiple coils is the need for shimming over an extended volume. Here, the experiment was intended for relaxometry including the measurement of a single ^{19}F signal. For this purpose, a typical line width of ~1 ppm as seen in Figure 2c-f is sufficient. Homogeneity could potentially be improved by shimming techniques for multiple coils, as well as by magnetic susceptibility matching of coils and flow cells.

The applicability of multiplexed D-DNP NMR can be extended to screening multiple ligands in one spectrum or to chemical shift based functional assays.[26] ^{19}F NMR detection offers the benefit of avoiding the need to suppress a large signal of hyperpolarized water protons. Screening methods based on polarization transfer from hyperpolarized water would also be compatible with the multiplexed system.[27] The multiplexed D-DNP approach can be used for other experiments that involve multiple measurements on the same sample with variations of experimental parameters. Such experiments would be inefficient with a conventional D-DNP instrumentation requiring multiple dissolutions. Examples include NMR based titrations or relaxation dispersion measurements that require multiple pulsing

delays.[28] Another approach to high-throughput D-DNP NMR has previously been described, which enables polarization of multiple different sample aliquots simultaneously and dissolving each sample independently.[13–16] The multiplexing method described here could also be combined with this approach to further increase the efficiency of D-DNP NMR experiments. Lastly, similar multiplexed flow NMR systems may be applicable to the measurements without hyperpolarization, such as in screening of protein-ligand interactions.

4. Conclusions

Using a multi-channel flow NMR system, we have demonstrated that the throughput of D-DNP NMR experiments can be improved by four times. The system was applied to determine the binding affinities of two non-fluorinated ligands from concentration-dependent R_2 relaxation measurements, using competitive binding with a fluorinated reporter ligand. From a single hyperpolarization experiment, a titration curve of the ligand under investigation could be obtained. Without altering the sample concentrations, it was possible to accurately measure the binding affinities of the two ligands, which differ 10-fold. Further, it was evaluated that this method permits to determine K_D in a range over three orders of magnitude under the experimental conditions examined. Besides the advantages brought by the increased throughput, the described screening method benefits from the dramatically enhanced signal intensity by hyperpolarization. It allowed to reduce the protein concentration to a few μM in a stock solution, and several hundred nM was sufficient for the measurements. These required sample concentrations are compatible with targeting proteins that are difficult to express or poorly soluble.

Supplementary Material

Refer to Web version on PubMed Central for supplementary material.

Acknowledgments

Financial support from the National Institutes of Health (Grant R21-GM107927) is gratefully acknowledged.

References

(1). Ardenkjær-Larsen JH; Fridlund B; Gram A; Hansson G; Hansson L; Lerche MH; Servin R; Thaning M; Golman K Increase in Signal-to-Noise Ratio of > 10,000 Times in Liquid-State NMR. PNAS 2003, 100 (18), 10158–10163. [PubMed: 12930897]

(2). Zhang G; Hilty C Applications of Dissolution Dynamic Nuclear Polarization in Chemistry and Biochemistry. Magnetic Resonance in Chemistry 2018.

(3). Duckett SB; Mewis RE Application of *Para* Hydrogen Induced Polarization Techniques in NMR Spectroscopy and Imaging. Accounts of Chemical Research 2012, 45 (8), 1247–1257. [PubMed: 22452702]

(4). Hovener J; Pravdivtsev AN; Kidd B; Bowers CR; Glöggler S; Kovtunov KV; Plaumann M; Katz-Brull R; Buckenmaier K; Jerschow A; et al. Parahydrogen-Based Hyperpolarization for Biomedicine. Angewandte Chemie 2018.

(5). Jensen PR; Meier S; Ardenkjær-Larsen JH; Duus JØ; Karlsson M; Lerche MH Detection of Low-Populated Reaction Intermediates with Hyperpolarized NMR. Chemical Communications 2009, No. 34, 5168. [PubMed: 20448982]

(6). Duckett SB; Newell CL; Eisenberg R Observation of New Intermediates in Hydrogenation Catalyzed by Wilkinson's Catalyst, RhCl(PPh3)3, Using Parahydrogen-Induced Polarization. Journal of the American Chemical Society 1994, 116 (23), 10548–10556.

(7). Lepre CA; Moore JM; Peng JW Theory and Applications of NMR-Based Screening in Pharmaceutical Research. Chem. Rev 2004, 104 (8), 3641–3676. [PubMed: 15303832]

(8). Platzer G; Okon M; McIntosh LP PH-Dependent Random Coil 1H, 13C, and 15N Chemical Shifts of the Ionizable Amino Acids: A Guide for Protein PK a Measurements. Journal of Biomolecular NMR 2014, 60 (2–3), 109–129. [PubMed: 25239571]

(9). Dubois BW; Evers AS Fluorine-19 NMR Spin-Spin Relaxation (T2) Method for Characterizing Volatile Anesthetic Binding to Proteins. Analysis of Isoflurane Binding to Serum Albumin. Biochemistry 1992, 31 (31), 7069–7076. [PubMed: 1643040]

(10). Furukawa A; Konuma T; Yanaka S; Sugase K Quantitative Analysis of Protein–Ligand Interactions by NMR. Progress in Nuclear Magnetic Resonance Spectroscopy 2016, 96, 47–57. [PubMed: 27573180]

(11). Sugase K; Dyson HJ; Wright PE Mechanism of Coupled Folding and Binding of an Intrinsically Disordered Protein. Nature 2007, 447 (7147), 1021–1025. [PubMed: 17522630]

(12). Lee Y Dissolution Dynamic Nuclear Polarization–Enhanced Magnetic Resonance Spectroscopy and Imaging: Chemical and Biochemical Reactions in Nonequilibrium Conditions. Applied Spectroscopy Reviews 2016, 51 (3), 210–226.

(13). Batel M; Krajewski M; Weiss K; With O; Däpp A; Hunkeler A; Gimersky M; Pruessmann KP; Boesiger P; Meier BH; et al. A Multi-Sample 94 GHz Dissolution Dynamic-Nuclear-Polarization System. J. Magn. Reson 2012, 214 (1), 166–174. [PubMed: 22142831]

(14). Crémillieux Y; Goutailler F; Montcel B; Grand D; Vermeulen G; Wolf P-E A Super-Wide Bore DNP System for Multiple Sample Polarization: Cryogenic Performance and Polarization at Low Temperature. Applied Magnetic Resonance 2012, 43 (1–2), 167–180.

(15). Hu S; Larson PEZ; VanCriekinge M; Leach AM; Park I; Leon C; Zhou J; Shin PJ; Reed G; Keselman P; et al. Rapid Sequential Injections of Hyperpolarized [1–13C]Pyruvate in Vivo Using a Sub-Kelvin, Multi-Sample DNP Polarizer. Magnetic Resonance Imaging 2013, 31 (4), 490–496. [PubMed: 23107275]

(16). Krajewski M; Wespi P; Busch J; Wissmann L; Kwiatkowski G; Steinhauser J; Batel M; Ernst M; Kozerke S A Multisample Dissolution Dynamic Nuclear Polarization System for Serial Injections in Small Animals: Multisample Dissolution DNP Polarizer for Small Animals. Magnetic Resonance in Medicine 2017, 77 (2), 904–910. [PubMed: 26900678]

(17). Kim Y; Hilty C Affinity Screening Using Competitive Binding with Fluorine-19 Hyperpolarized Ligands. Angew. Chem. Int. Ed 2015, 54 (16), 4941–4944.

(18). Kim Y; Liu M; Hilty C Parallelized Ligand Screening Using Dissolution Dynamic Nuclear Polarization. Anal. Chem 2016.

(19). Kodibagkar VD; Conradi MS Remote Tuning of NMR Probe Circuits. Journal of Magnetic Resonance 2000, 144 (1), 53–57. [PubMed: 10783273]

(20). Meiboom S; Gill D Modified Spin-Echo Method for Measuring Nuclear Relaxation Times. Review of Scientific Instruments 1958, 29 (8), 688–691.

(21). Wennerström H Nuclear Magnetic Relaxation Induced by Chemical Exchange. Molecular Physics 1972, 24 (1), 69–80.

(22). Palmer AG; Kroenke CD; Patrick Loria J Nuclear Magnetic Resonance Methods for Quantifying Microsecond-to-Millisecond Motions in Biological Macromolecules. In Methods in Enzymology; Elsevier, 2001; Vol. 339, pp 204–238. [PubMed: 11462813]

(23). Lee Y; Zeng H; Ruedisser S; Gossert AD; Hilty C Nuclear Magnetic Resonance of Hyperpolarized Fluorine for Characterization of Protein–Ligand Interactions. J. Am. Chem. Soc 2012, 134 (42), 17448–17451. [PubMed: 23020226]

(24). Wang Z-X An Exact Mathematical Expression for Describing Competitive Binding of Two Different Ligands to a Protein Molecule. FEBS Letters 1995, 360 (2), 111–114. [PubMed: 7875313]

(25). Markwardt F; Landmann H; Walsmann P Comparative Studies on the Inhibition of Trypsin, Plasmin, and Thrombin by Derivatives of Benzylamine and Benzamidine. European Journal of Biochemistry 1968, 6 (4), 502–506. [PubMed: 5701967]

(26). Vulpetti A; Hommel U; Landrum G; Lewis R; Dalvit C Design and NMR-Based Screening of LEF, a Library of Chemical Fragments with Different Local Environment of Fluorine. J. Am. Chem. Soc 2009, 131 (36), 12949–12959. [PubMed: 19702332]

(27). Chappuis Q; Milani J; Vuichoud B; Bornet A; Gossert AD; Bodenhausen G; Jannin S Hyperpolarized Water to Study Protein–Ligand Interactions. J. Phys. Chem. Lett 2015, 6 (9), 1674–1678. [PubMed: 26263332]

(28). Liu M; Kim Y; Hilty C Characterization of Chemical Exchange Using Relaxation Dispersion of Hyperpolarized Nuclear Spins. Analytical Chemistry 2017, 89 (17), 9154–9158. [PubMed: 28714674]

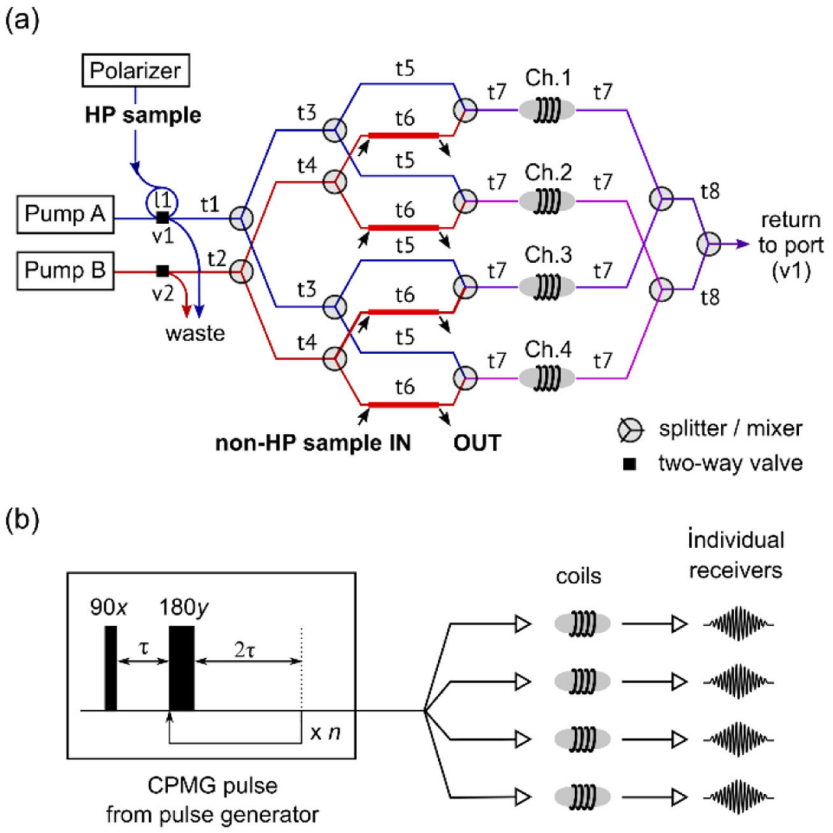

Figure 1.

(a) Flow path designed for simultaneous injection of four hyperpolarized samples into NMR flow cells. Non-HP reagents are independently admixed to each channel. t1: 152 cm, t2: 15 cm, t3 and t4: 5 cm, t5: 12 cm, t6: 20 cm, t7: 65 cm, and t8: 15 cm (b) Schematic of pulse transmission and signal reception for simultaneous NMR measurements with multiple channels. A CPMG pulse sequence employed for R_2 relaxation measurement is shown.

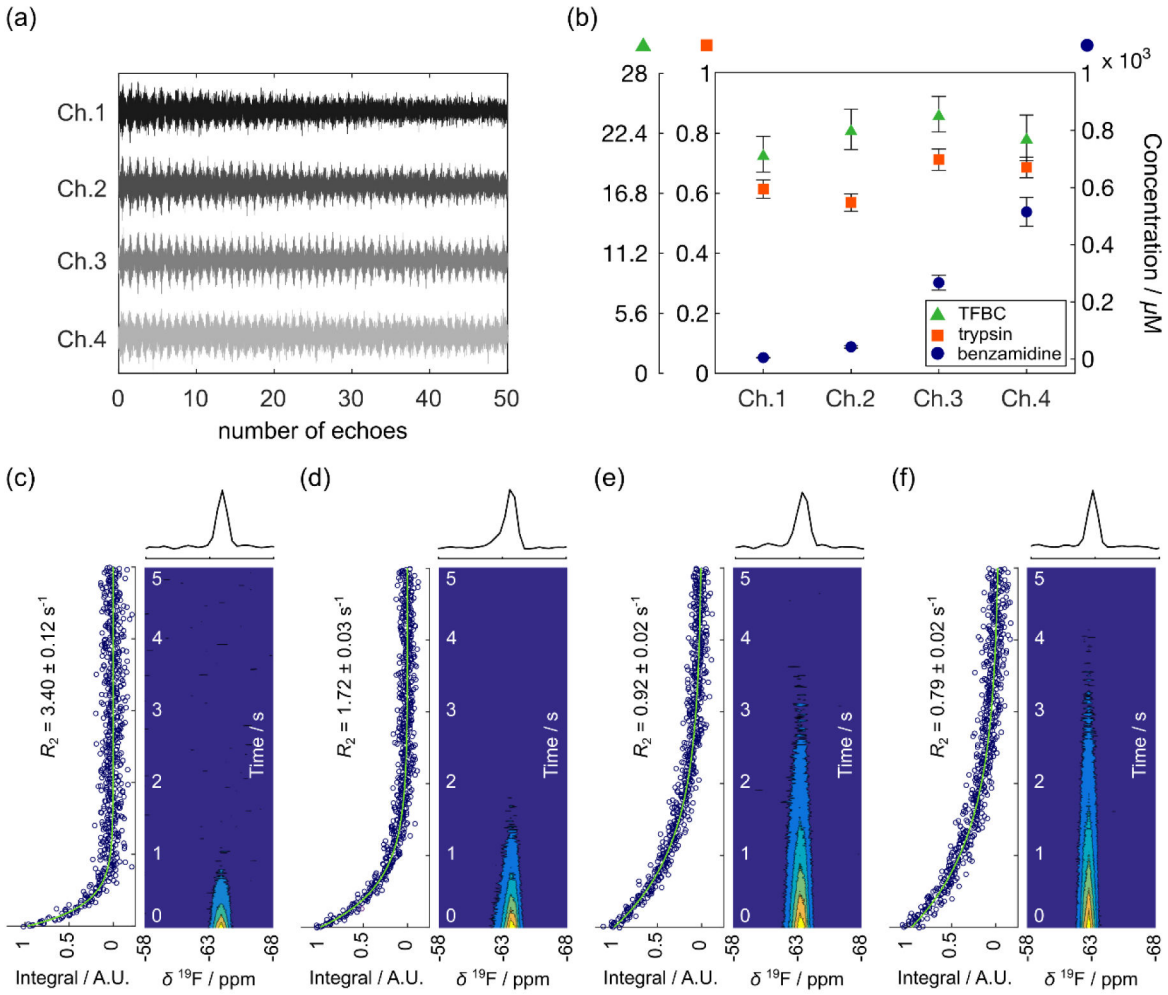

Figure 2.

(a) First 50 spin-echoes acquired from the four simultaneous measurements of concentration-dependent relaxation rates of hyperpolarized reporter ligand (TFBC) in the presence of trypsin and the competing ligand, benzamidine. (b) Final concentrations determined for TFBC, trypsin, and benzamidine in the measurements shown in (a). (c)-(f) Contour plots of chemical shift resolved CPMG spectra obtained from Ch1 – Ch4 (from left to right). First 625 spectra (0 ~ 5 s) are shown. The first spectrum from each dataset is shown on top of the contour plot. The integrated signals are plotted with a fitted curve (green) next to the contour plot.

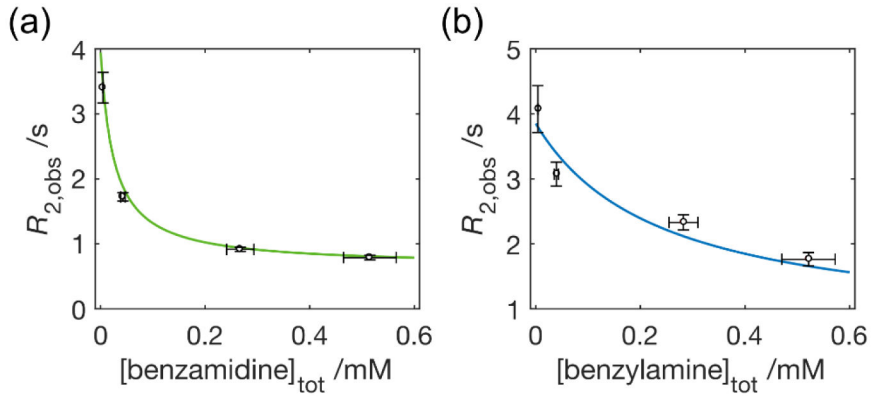

Figure 3.

R_2 plots obtained from the relaxation measurements for benzamidine (a) and benzylamine (b). The curves represent the calculated relaxation rates using the fitted K_D of 21.6 μM and 205 μM for benzamidine and benzylamine, respectively, in combination with the average concentrations of trypsin and TFBC from the four channels. The error bars represent the 95% confidence intervals associated with the measured $R_{2,obs}$ (along the y-axis) and 5% error of the measured concentrations for the competing ligands (along the x-axis)

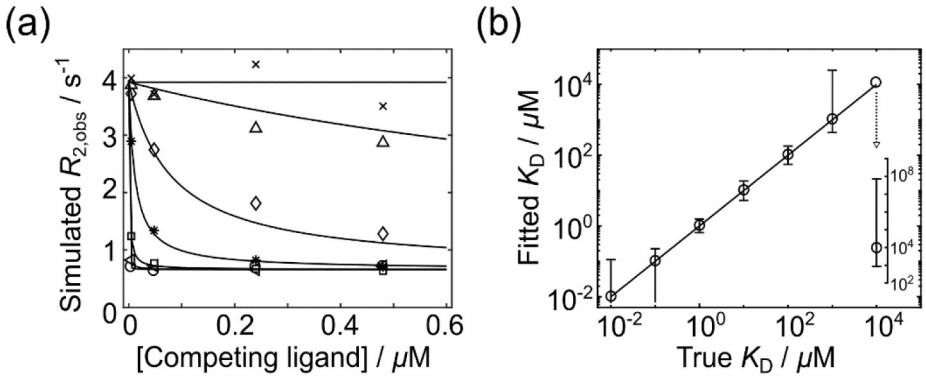

Figure 4.

(a) Random sets of simulated $R_{2,obs}$ values generated for each case of the competing ligand with $K_D = 10^{-2}$, 10^{-1}, 10^{0}, 10^{1}, 10^{2}, 10^{3}, and 10^{4} μM. For the simulations, the concentrations of reporter ligand, trypsin, and competing ligand were 22.3 μM, 0.62 μM, and [4.8, 48, 240, 480] μM; $R_{2,f} = 0.66$ s^{-1}, $R_{2,b} = 841$ s^{-1}, reporter ligand $K_D = 142$ μM. The curves represent the best fits to simulated data points. (b) Simulation results. Median values of the K_D distributions resulting from 10^4 simulated datasets ('Fitted K_D') are plotted versus the corresponding values of true K_D. The error bars indicate 95% confidence intervals of the simulated K_D distributions. The lower end of the error bar for $K_D \leq 10^{-1}$ μM extends to $K_D = 0$, which could not be drawn in the plot.

Table 1.

Sample dilution factors measured for HP and non-HP samples after injection into the flow cells.

		Ch.1	Ch.2	Ch.3	Ch.4	Average
HP sample	DF*	489 ± 40	439 ± 37	414 ± 28	455 ± 44	450 ± 32
	DF ratio	1.2	1.1	1.0	1.1	
Non-HP sample	DF	8.1 ± 0.6	9.1 ± 0.5	6.8 ± 0.2	7.3 ± 0.3	7.8 ± 1.0
	DF ratio	1.2	1.3	1.0	1.1	

*DF stands for dilution factor, defined by the ratio of initial to final sample concentrations.

Table 2.

Transverse relaxation rates measured for free ($R_{2,f}$) and bound ($R_{2,b}$*) ligands

	Ch.1	Ch.2	Ch.3	Ch.4	Average
$R_{2,f}$ / s^{-1}	0.67 ± 0.02	0.65 ± 0.02	0.66 ± 0.02	0.65 ± 0.01	0.66 ± 0.02
$R_{2,b}$* / s^{-1}	900 ± 90	798 ± 79	872 ± 65	794 ± 75	841 ± 82

Table 3.

The K_D estimates obtained from the concentration-dependent R_2 measurements and the associated error ranges from MonteCarlo simulations.

Ligand		K_D (μM)[a]	Literature values (μM)
Benzamidine	Trial 1	21.6, (12.0, 36.1)	35,[25] 16 ± 2,[17] (8.3, 19.6)[b,18]
	Trial 2	23.0, (14.1, 36.1)	
	Trial 3	22.2, (12.4, 36.7)	
Benzylamine	Trial 1	205, (136, 327)	300,[25] 218 ± 43,[17] (151, 328)[b,18]
	Trial 2	220, (141, 362)	
	Trial 3	215, (142, 351)	

[a]The first value indicates K_D (μM) obtained from the fitting of $R_{2,obs}$ datasets, and the following values in the parenthesis represent the central 95% of the K_D distributions yielded from the simulations.

[b]The values in the parenthesis represent 95% confidence intervals of K_D distributions determined from error analysis using MonteCarlo method.